Final Report

Bio-Electro-Mechanical Energy Conversion Technology for Future Wearable Electronics

Alireza Khaligh

A PhD Student (Mr. Peng Zeng) has been assigned to this project. Mr. Peng Zeng has been involved in analyzing the hybrid piezoelectric and electromagnetic energy harvesting topologies. The focus has been in developing *Mesoscale* (centimeter sized) energy harvesting systems to produce power from human normal activities. The up and down motion of the center of gravity as a potential energy source has been studied.

Fig. 1 presents the structure of the proposed hybrid piezoelectric (PZT) and permanent magnet energy scavenging topology, for the linear up and down motion of the center of gravity. In this system, the windings are distributed on the stator and permanent magnets (PM) are placed on the moving mass. The moving part is connected to a piezoelectric (PZT) beam through springs on both sides. In this structure, magnetic structure and PZT beams around the moving mass are the primary sources of energy. The moving mass is connected to four serpentine-piezoelectric springs on four sides. The copper coil is fixed in the middle of the moving mass, which significantly improves the output voltage. The proposed design is primarily for body's center of gravity up and down motion; however, with slight variations in the structure, it can be designed for arm, limb, knee, and foot horizontal linear motions.

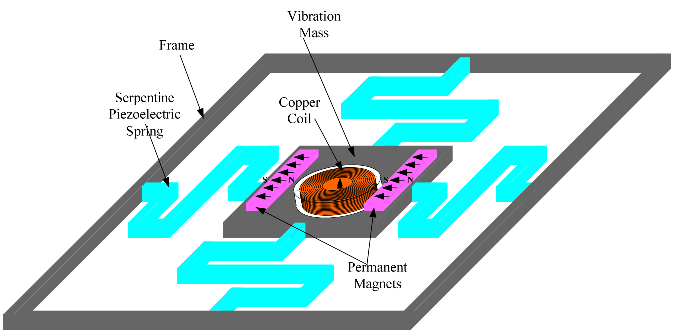

Fig. 1. Proposed hybrid piezoelectric and permanent magnet energy scavenging topology.

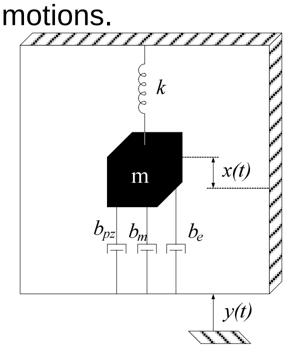

Fig. 2. General structure of a vibration to electricity electromagnetic converter.

A. Electromagnetic Conversion

A model has been developed to predict the amount of power, which can be generated from PM conversion part (Fig. 2). Based on the model

$$m\frac{d^2x(t)}{dt^2} + (b_e + b_m + b_{pz})\frac{dx(t)}{dt} + kx(t) = -m\frac{d^2y(t)}{dt^2} \qquad (1)$$

where b_e is the electrically induced damping coefficient, b_m is the mechanical damping coefficient, $x(t)$ is the spring deflection and y is the input displacement, m is the proof mass, and k is the spring constant. The electrical damping factor is, $b_e = \frac{F}{v} = \frac{nBli}{v} = \frac{nBl\frac{V}{R}}{v} = \frac{nBl\frac{nBlv}{R}}{v} = \frac{(nBl)^2}{R}$ and the piezoelectric damping factor is

$$b_{pz} = \frac{2m\omega_n^2 k_{31}^2}{\sqrt{\omega_n^2 + \frac{1}{(R_L C_p)^2}}}.$$

where k_{31} is the piezoelectric coupling coefficient $k_{31}^2 = \frac{d_{31}^2 Y_p}{\varepsilon_p}$, C_p is the capacitance of the piezoelectric bender, R_L is the load resistance, d_{31} is the piezoelectric constant for 31 mode, Y_p is the Young's modulus of piezoelectric material, and ε_p is the dielectric constant of piezoelectric material The maximum output power, when the resonant frequency of the spring mass system matches the input frequency, is,

$$|P| = \frac{m\zeta_e \omega_n^3}{4\varsigma_T^2}|Y|^2 \qquad (2)$$

B. *Piezoelectric Conversion*

The structure of piezoelectric conversion part and its geometric dimensions are illustrated in Fig. 3. The equivalent circuit model of such vibration-induced piezoelectric cantilever generator is proposed in Fig. 4.

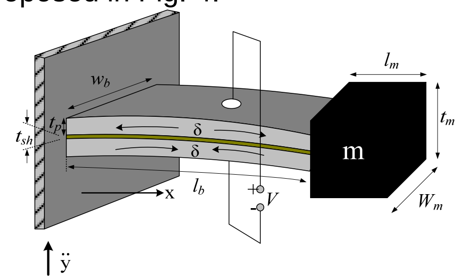

Fig. 3. The geometric dimention of the piezoelectric cantilever.

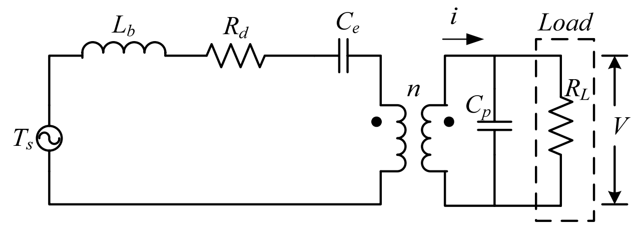

Fig. 4. Equivalent circuit model of the vibration-induced piezoelectric bender generator.

The equivalent inductor, L_b, represents the inertia of the bender, which mainly comes from the end mass *m*. The equivalent resistor, R_d, represents the bender's mechanical damping during vibration. The equivalent capacitor, C_e, represents the mechanical stiffness of the bender. T_s is the equivalent stress source that represents the stress generated by the drive of input vibration. The transformer with *n* equivalent turns ratio represents the coupling between mechanical stress and electrical filed. C_p is the capacitance of the piezoelectric bender. l_m, l_e, l_b, w_b, t_p, t_{sh}, *b* are geometric parameters of the cantilever beam, where l_e is the length of electrode on piezoelectric layer, $b = \frac{t_p + t_{sh}}{2}$ and other parameters are clearly illustrated in Fig. 3. $\gamma_s = \frac{Y_{sh}}{Y_p}$ is the ratio of the Young's modulus for the center shim (Y_{sh}) to the Young's modulus for the piezoelectric material (Y_p). The total damping ratio is defined as $\zeta_T = \frac{b_T}{2\omega_n m}$ where b_T is the sum of mechanical and electrical damping coefficients. For sinusoidal excitation vibration, $A_{in} = Y_0\omega^2$. Substituting $s = j\omega$ and $k_{31}^2 = \frac{d_{31}^2 Y_p}{\varepsilon_p}$, the generated voltage can be expressed as

$$V_{PZT} = \frac{-j\omega^3 \frac{2Y_p d_{31} t_p}{\varepsilon_p} \frac{Y_0}{k_2}}{\left[\frac{\omega_n^2}{R_L C_p} - \left(\frac{1}{R_L C_p} + 2\zeta_T \omega_n\right)\omega^2\right] + j\omega\left[(1+k_{31}^2)\omega_n^2 + \frac{2\zeta_T \omega_n}{R_L C_p} - \omega^2\right]} \qquad (3)$$

When the resonant frequency ω_n is designed to be equal to the driving vibration frequency, ω, equation (3) will be simplified to

$$V_{PZT} = \frac{-j\omega^2 \frac{2Y_p d_{31} t_p}{\varepsilon_p} \frac{Y_0}{k_2}}{j\left(k_{31}^2\omega^2 + \frac{2\zeta_T \omega}{R_L C_p}\right) - (2\zeta_T \omega^2)} \qquad (4)$$

The transferred power to the resistive load is

$$P_{PZT} = \frac{|V_{PZT}|^2}{2R_L} = \frac{2(Y_0 C_p \omega)^2 \left(\frac{Y_p d_{31} t_p}{k_2 \varepsilon_p}\right)^2}{4\zeta_T k_{31}^2 C_p \omega + (4\zeta_T{}^2 + k_{31}^4)(C_p\omega)^2 R_L + \frac{4\zeta_T{}^2}{R_L}} \quad (5)$$

The maximum transferred power through a single piezoelectric cantilever beam, based on eq. (5), is achievable for minimum value of the denominator in eq. (5). Minimum of denominator in eq. (5), can be achieved when R_L meets the equation of $(4\zeta_T{}^2 + k_{31}^4)(C_p\omega)^2 R_L = \frac{4\zeta_T{}^2}{R_L}$. Therefore $R_{L,opt}$ would be, $R_{L,opt} = \frac{1}{\omega C_p} \frac{2\zeta_T}{\sqrt{4\zeta_T{}^2 + k_{31}^4}}$. As a result,

$$P_{PZT,\max} = \frac{1}{2} \frac{\omega C_p \left(\frac{Y_0 t_p}{k_2}\right)^2 \frac{Y_p}{\varepsilon_p}}{\zeta_T \left[\sqrt{\left(\frac{\zeta_T}{k_{31}^2}\right)^2 + 1} + 1\right]} \quad (6)$$

C. Results

A mesoscale hybrid topology has been designed. Table 1 presents the parameters of the proposed structure in Fig. 1. Based on the design parameters, presented in Table 1, the output power of the electromagnetic and piezoelectric conversion parts of the proposed structure are approximately 37 mW and 6 mW, respectively.

TABLE 1. Parameters of the structure in Fig. 1.

Center-of-mass vibration frequency	$f = 2Hz$
Center-of-mass vibration amplitude	$Y_0 = 3\ cm$
Flux density	$B = 0.5\,\text{T}$
Length of one coil side	$l = 1\,\text{cm}$
Number of coil turns	n=350
Load resistor of coil	$R_{coil} = 10\ \Omega$
Mechanical damping ratio	$\varsigma_m = 0.0137$
PZT charge coefficient	$d_{31} = -175 \times 10^{-12}$ C/N
PZT voltage coefficient	$g_{31} = 0.011 V \cdot m / N$
PZT dielectric constant	$\varepsilon = 1700\varepsilon_0$
PZT Young's modulus	$Y_{PZT} = 63\ GPa$
PZT density	$\rho_{PZT} = 7.75\ g/cm^3$
Brass Young's modulus	$Y_{Brass} = 103.5\ GPa$
Brass density	$\rho_{Brass} = 8.4\ g/cm^3$
Frame length	$L_f = 7cm$
Frame width	$W_f = 7cm$
Frame thickness	$H_f = 0.4cm$
Length of each serpentine spring	$l_b = \frac{l}{2} = 19.6\ cm$
Width of serpentine spring	$w_b = 0.4\ mm$
Thickness of PZT layer	$t_p = 0.18\,mm$
Thickness of elastic layer	$t_{sh} = 0.04\,mm$
Length of proof mass	$l_m = 3.5\,cm$
Width of proof mass	$w_m = 3.5\,cm$
Thickness of proof mass	$t_m = 0.4\ cm$
Weight of end mass (PZT material)	$m = 38\,g$
Length of electrode	$l_e = l_b = 19.6\ cm$
Resonant frequency of the bender	$f_n = 2.0Hz$

I. Conclusion

In this project a novel hybrid topology to harvest energy from human normal motion has been proposed. The analytical modeling of the electromagnetic and piezoelectric energy conversion parts are presented in detail. It is shown that 43 mW output power can be extracted from the hybrid topology from up and down motion of center of gravity. Presented results demonstrate the advantages of hybrid topologies, as enabling technology for future wearable electronic devices.

Two referred papers have been published based on this research. In addition two proposals have been submitted to the NSF based on the outcomes of this project.

1- A. Khaligh, P. Zeng, X. Wu, and Y. Xu, "Hybrid energy harvesting topology for human-powered mobile electronics," in *Proc. 34th Annual Conference of the IEEE Industrial Electronics Society,* Nov. 2008, Orlando, FL.

2- X. Wu, A. Khaligh, and Y. Xu, "Modeling, design, and optimization of hybrid electromagnetic and piezoelectric MEMS energy scavengers," in *Proc. IEEE Custom Integrated Circuits Conference (CICC)*, Sept. 2008, San Jose, Ca.